PAPER

Check for updates

Biorenewable rosin derived benzocyclobutene resin: a thermosetting material with good hydrophobicity and low dielectric constant†

Fei Fu,[ab] Dan Wang,[ac] Minggui Shen, [iD] *[ac] Shibin Shang,[ac] Zhanqian Song[a] and Jie Song[d]

Development of bio-based polymers has been promoted by the growing concerns about the long-term sustainability and negative environmental footprint of petroleum-based polymer materials. A new monomer containing benzocyclobutene and allyl units has been developed by using rosin as the feedstock. The structure of the monomer was characterized by elemental analysis, MS, FT-IR and NMR spectroscopy. The monomer could be converted to the polymer via thermal ring-opening polymerization which was characterized via FT-IR, thermogravimetric analysis (TGA), atom force microscopy (AFM) and so on. The polymer showed good dielectric properties and hydrophobicity with an average dielectric constant of 2.51 in a range of frequencies from 0.1 to 18 MHz and a water contact angle of 106°. In addition, the polymer with other comprehensive performances exhibited a 5% weight loss temperature of 406 °C, a surface roughness (R_a) of 0.658 nm in a 5.0 × 5.0 μm^2 area, hardness and Young's modulus of 0.283 and 3.542 GPa, and storage modulus of 11.46 GPa at 30 °C. These data suggest that the polymer may have potential application in electronics and microelectronics.

Introduction

With the rapid development of the military, aerospace and microelectronic industries, high performance polymers are urgently needed. Benzocyclobutene resins, as one family of high performance polymers, have attracted lots of attention in recent years.[1–5] The monomer benzocyclobutene, in certain circumstances, could undergo ring-opening reaction to provide reactive o-quinodimethane, which could undergo dimerization and polymerization, or react with a dienophile to form a Diels–Alder adduct.[1,3,4,6–11] Generally, the resulting benzocyclobutene resins show excellent dielectric properties and thermal stability, and

low water absorption and thermal expansion coefficient.[12] Correspondingly, the benzocyclobutene resins have been widely used in the fields of aerospace, electronics and microelectronics, as enameled wire varnish, large scale integrated circuits, composite materials, etc.[13–16] Due to the increasingly demanding of the exceptional intermediate layer dielectric materials containing excellent dielectric properties, good hydrophobicity and thermal stability, the benzocyclobutene resins would be further functionalized to satisfy the specific requirement of the performance in some cases.[17–19] For example, introducing the siloxane group, fluorine-containing group and low polarity bulky group would result in improvements of the dielectric properties and thermal stability.[5,17–21] However, most of them reveal some defects, for example, the siloxane-based benzocyclobutene resins show excellent thermal stability but they can not lower the dielectric constant very well.[10,12,22] The fluorinated benzocyclobutene resins usually have low dielectric constant, but they always show poor adhesion to metal and poor dimensional stability.[21] Increasing the free volume by introducing bulky groups into the polymers can decrease the dielectric constant of the polymers.[17] Therefore, introducing the low polar bulky functional groups into the polymer turns into the feasible approach for designing and preparation of excellent dielectric materials.[21]

Recently, polymeric materials derived from renewable biomasses such as lignin, cellulose and rosin have received more attention due to their depletion of petroleum resources and the demand of environmental protection.[23–28] Rosin, a well-

[a]Institute of Chemical Industry of Forest Products, Chinese Academy of Forestry, Key Laboratory of Biomass Energy and Material, National Engineering Laboratory for Biomass Chemical Utilization, Key and Open Laboratory of Forest Chemical Engineering, State Forestry Administration, Nanjing 210042, Jiangsu Province, China. E-mail: mingguishen@163.com; Fax: +86-25-85482452; Tel: +86-25-85482452

[b]Co-Innovation Center of Efficient Processing and Utilization of Forest Resources, Nanjing Forestry University, Nanjing 210037, People's Republic of China

[c]Institute of New Technology of Forestry, Chinese Academy of Forestry, Beijing 100091, China

[d]Department of Chemistry and Biochemistry, University of Michigan-Flint, Flint, Michigan 48502, USA

known biomass with a large hydrogenated phenanthrene ring structure, has been successfully converted to numbers of polymeric materials with excellent thermal, mechanical and hydrophobic properties.[29–37] Wang *et al.* introduced rosin into pressure-sensitive adhesive by emulsion polymerization in order to improve the mechanical properties of the copolymer.[23] El-Ghazawy *et al.* synthesized a rosin-based epoxy resin used in coatings which showed good thermal stability.[32] Xu *et al.* prepared a rosin-based waterborne polyurethane, and the introduction of rosin structure enhanced the hydrophobicity of the material.[36] Moreover, the hydrogenated phenanthrene ring structure is bulky, rigid, hydrophobic and low-polar,[23,31] so the introduction of the structure might improve the thermal stability, hydrophobicity and dielectric properties of benzocyclobutene resins.

In this work, a rosin-based benzocyclobutene monomer had been synthesized by using dehydroabietic acid as raw material. According to the benzocyclobutene reaction mechanism, the monomer containing benzocyclobutene and allyl units could be used as a precursor for the preparation of high performance materials, which exhibited good thermal stability, hydrophobicity and dielectric properties (Scheme 1). These results indicate that the polymer is suitable as encapsulation resin or dielectric material in the field of electronics and microelectronics.

Experimental

Materials

Dehydroabietic acid (DA) was obtained from Wuzhou Chemical Co., Ltd. Benzocyclobutene-4-boronic acid was purchased from Chemtarget Technologies Co., Ltd. *N*-Bromosuccinimide (NBS), tripotassium phosphate, Tetrakis(triphenylphosphine)palladium(0), allyl bromide, potassium carbonate and azodiisobutyronitrile (AIBN) were obtained from Aladdin Industrial Corporation. Ethanol,

acetonitrile, acetone, xylene, ethyl acetate and petroleum ether were purchased from Nanjing Chemical Reagent Co., Ltd. All chemicals were used without purification.

Measurements

^{1}H NMR and ^{13}C NMR spectra were recorded on a Bruker 400 spectrometer using TMS as internal standard with DMSO as a solvent at room temperature. Mass spectra (MS) for compounds were recorded on Waters Q-TOF Micro™ spectrometer and 5973 Network (Agilent) Mass Selective Detector. FT-IR spectra were carried out on a Thermo Scientific Nicolet IS10 spectrometer (Nicolet) by ATR (attenuated total reflectance). Differential scanning calorimetry (DSC) was run using a PerkinElmer Diamond Differential Scanning Calorimeter with temperature increased at a rate of 10 °C min^{-1} in N$_2$ atmosphere. Thermogravimetric analysis (TGA) was performed on a TG209F1 (NETZSCH, Germany) apparatus with a heating rate of 10 °C min^{-1} in N$_2$ atmosphere. The contact angle of the cured resin was measured at room temperature using a sessile drop method on a dynamic contact angle measurement instrument (JC2000C). Deionized water was selected as the testing liquid. Surface toughness of the polymer film was measured by atom force microscopy (AFM) on a Shimadzu SPM-9600 (Japan). The dielectric constant and dielectric loss of the cured resin were measured in a range of frequencies from 0.1 to 18 MHz at room temperature using a 4294A Precision Impedance Analyzer (Agilent). The mechanical properties of the cured resin were measured on a nanoindentation system called UNHT (Anton Paar). The phase structure of as-prepared product was characterized with X-ray diffraction (XRD, Bruker D8 advance with Cu Kα λ = 1.5418 Å). The scans were taken within the 2θ range between 5° and 40° and operated at an accelerating voltage of 40 kV and an emission current of 40 mA. Dynamic Mechanical Analysis (DMA) of samples was performed in stretching mode
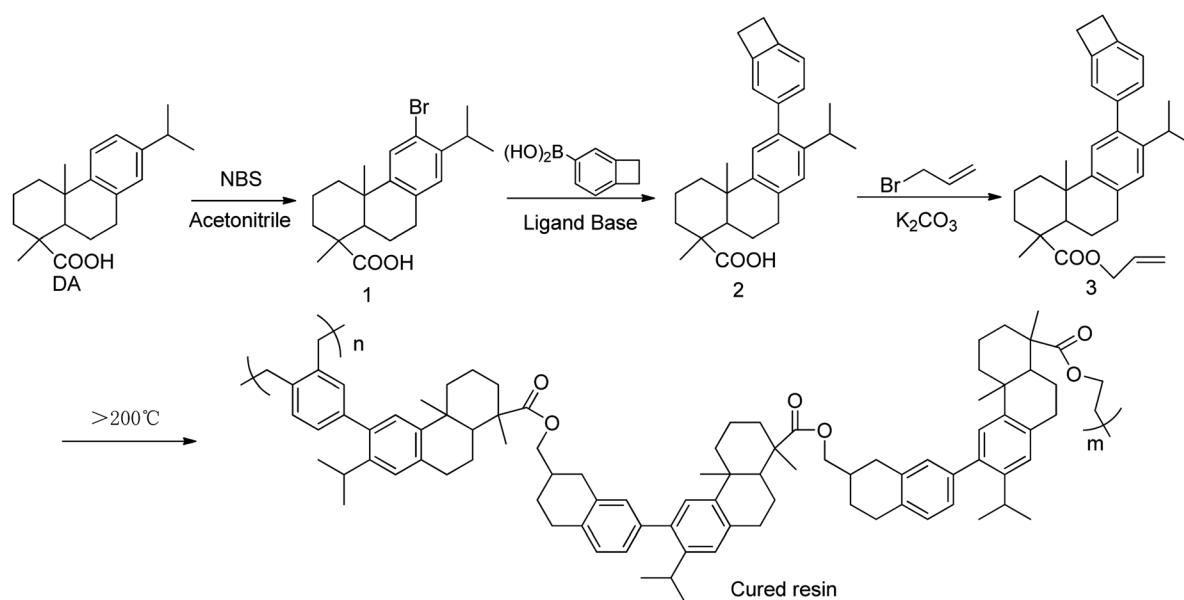
Scheme 1 Procedure for the synthesis of the new monomer and polymer.

using a DMA Q800 (TA, USA). The frequency was set at 1 Hz, and each sample was scanned from 30 to 300 °C at a heating rate of 3 °C min^{-1}. Elemental analysis was performed as C/H analyses on an elemental analyzer (PE-2400, PE, USA).

Synthesis of Compound 1

Dehydroabietic acid (0.017 mol, 5.00 g) was dissolved in anhydrous acetonitrile (337 mL), and NBS (0.031 mol, 5.54 g) was added. Then the mixture was reacted in darkness at room temperature for 24 h. The mixture was suction filtered, yielding a white solid that was dissolved in ethyl acetate (50 mL). The organic phase was then washed with water (50 mL, ×3) and dried over anhydrous Na_2SO_4. After filtration and concentration, Compound 1 was purified using column chromatography with a mixture of petroleum ether and ethyl acetate as the eluent (5 : 1, v/v). ^1H NMR (400 MHz, DMSO) δ 12.20 (s, 1H), 7.36 (s, 1H), 7.00 (s, 1H). ^{13}C NMR (101 MHz, DMSO) δ 179.24 (m), 149.21 (s), 143.23 (s), 134.51 (s), 127.95 (s), 127.20 (s), 120.79 (m), 46.23 (s), 44.24 (s), 37.48 (s), 36.53 (s), 36.13 (s), 31.92 (s), 28.89 (s), 24.55 (s), 22.68 (s), 22.59 (s), 20.77 (m), 18.02 (s), 16.30 (s). Anal. calcd. for $C_{20}H_{27}BrO_2$: C 63.33, H 7.17; found: C 64.22, H 7.10.

Synthesis of Compound 2

Under nitrogen atmosphere, Compound 1 (1.00 mmol, 0.379 g), benzocyclobutene-4-boronic acid (1.25 mmol, 0.185 g) and tripotassium phosphate (2.00 mmol, 0.425 g) were dissolved in an ethanol/water mixture (6 mL, 1 : 1, v/v). Then tetrakis(triphenylphosphine)palladium(0) (0.01 mmol, 0.0116 g) was added before the mixture was heated at 60 °C for 10 h. The mixture was cooled to room temperature and suction filtered with diatomite. The filtrate was then extracted with ethyl acetate (30 mL, ×2). The organic phases were combined, washed with water (50 mL, ×3), dried over anhydrous Na_2SO_4, filtered and concentrated to afford the crude product. Compound 2 was purified using column chromatography with a mixture of petroleum ether and ethyl acetate as the eluent (5 : 1, v/v). ^1H NMR (400 MHz, DMSO) δ 12.16 (s, 1H), 7.10 (d, J = 7.5 Hz, 1H), 7.02 (dd, J = 7.5, 0.9 Hz, 1H), 7.00 (s, 1H), 6.93 (s, 1H), 6.91 (s, 1H), 3.18 (s, 4H). ^{13}C NMR (101 MHz, DMSO) δ 179.35 (s), 146.27 (s), 144.87 (s), 143.43 (s), 142.46 (s), 140.55 (s), 138.94 (s), 133.51 (s), 127.71 (s), 125.42 (s), 125.26 (s), 123.19 (s), 122.01 (s), 46.33 (s), 44.58 (s), 37.70 (s), 36.33 (s), 36.23 (s), 29.16 (s), 29.04 (s), 28.85 (s), 28.34 (s), 24.77 (s), 24.19 (s), 23.99 (s), 21.09 (s), 18.09 (s), 16.32 (s). Anal. calcd. for $C_{28}H_{34}O_2$: C 83.54, H 8.51; found: C 82.55, H 8.96.

Synthesis of Monomer 3

Into a 100 mL three-necked round-bottom flask equipped with reflux condenser were charged Compound 2 (1.56 mmol, 0.680 g), K_2CO_3 (2.56 mmol, 0.216 g) and acetone (10 mL). A solution of allyl bromide (3.12 mmol, 0.377 g) dissolved in acetone (5.0 mL) was added dropwise at 50 °C. Then the mixture was refluxed at 70 °C for 12 h. The mixture was cooled to room temperature and filtered before being diluted with ethyl acetate (50 mL). The solution was washed with water (50 mL, ×3), dried

over anhydrous Na_2SO_4. After removal of the solvent, the crude product was obtained. Monomer 3 was purified using column chromatography with a mixture of petroleum ether and ethyl acetate as the eluent (10 : 1, v/v). ^1H NMR (400 MHz, DMSO) δ 7.09 (d, J = 7.5 Hz, 1H), 7.02 (s, 1H), 6.99 (s, 1H), 6.92 (s, 1H), 6.91 (s, 1H), 5.92 (ddd, J = 22.6, 10.7, 5.4 Hz, 1H), 5.30 (dd, J = 17.2, 1.5 Hz, 1H), 5.21 (dd, J = 10.5, 1.2 Hz, 1H), 4.56 (ddd, J = 27.4, 13.6, 5.4 Hz, 2H), 3.16 (s, 4H). ^{13}C NMR (101 MHz, DMSO) δ 177.00 (s), 146.06 (s), 144.85 (s), 143.43 (s), 142.54 (s), 140.52 (s), 139.03 (s), 133.38 (s), 132.78 (s), 127.68 (s), 125.43 (s), 125.30 (s), 123.17 (s), 121.99 (s), 117.64 (s), 64.58 (s), 47.00 (s), 44.73 (s), 37.59 (s), 36.41 (s), 36.15 (s), 29.16 (s), 29.03 (s), 28.85 (s), 28.34 (s), 24.85 (s), 24.15 (s), 23.98 (s), 21.12 (s), 18.00 (s), 16.27 (s). Anal. calcd. for $C_{31}H_{38}O_2$: C 84.12, H 8.65; found: C 83.46, H 8.90.

Preparation of benzocyclobutene polymers

Monomer 3 was placed in a glass mold filled with nitrogen. The mold was placed in a tube furnace for heating. Then the temperature was elevated and kept at 180 °C for 6.0 h, 210 °C for 1.0 h, 230 °C for 1.5 h, 250 °C for 1.5 h and 290 °C for 0.5 h, respectively. A completely cured sample was thus prepared, which was used to measure dynamic mechanical, dielectric properties and for nanoindentation tests.

A solution of Monomer 3 dissolved in xylene (35 mg mL^{-1}) was spin-coated on a monocrystalline silicon wafer to form a smooth film which was dried for 24 h at room temperature. The silicon wafer was placed into a tube furnace and heated stepwise at 180 °C/1.0 h, 210 °C/1.0 h, 230 °C/1.5 h, 250 °C/1.5 h and 290 °C/0.5 h. After cooling down to room temperature, the sample was used for the measurement of surface toughness.

Results and discussion

Synthesis and characterization

As shown in Scheme 1, the functional Monomer 3 was prepared *via* a three-step procedure by using dehydroabietic acid as the feedstock. The chemical structure of the monomer was confirmed by ^1H NMR, ^{13}C NMR, MS, FT-IR and elemental analysis. In its ^1H NMR spectrum (Fig. 1), the signals from 0.5 ppm to 3.0 ppm were all attributed to the protons attached on the hydrogenated phenanthrene ring;[38] the peaks at 5.92 ppm, 5.21–5.30 ppm and 4.56 ppm were assigned to the protons on the terminal $-CH_2-CH=CH_2$ groups; the signals from 6.91–7.09 ppm were all attributed to the protons attached on the benzene ring, and the characteristic peak at 3.16 ppm belonged to the protons on the four-membered ring of benzocyclobutene. FT-IR of Monomer 3 was shown in Fig. 2. As could be seen in Fig. 2, the absorption peaks at 1467, 934, 833 cm^{-1} were ascribing to the in-plane ring stretching vibration of C–H in the four-member ring of benzocyclobutene group;[17] the signals at 1644, 997, 907 cm^{-1} in Monomer 3, were assigned to the characteristic peak for allyl group. In addition, the characteristic peak for ester group was observed at 1710 cm^{-1}. ^1H NMR, ^{13}C NMR, MS of synthetic compounds were described in ESI.† Thus, all data were consistent with the proposed,
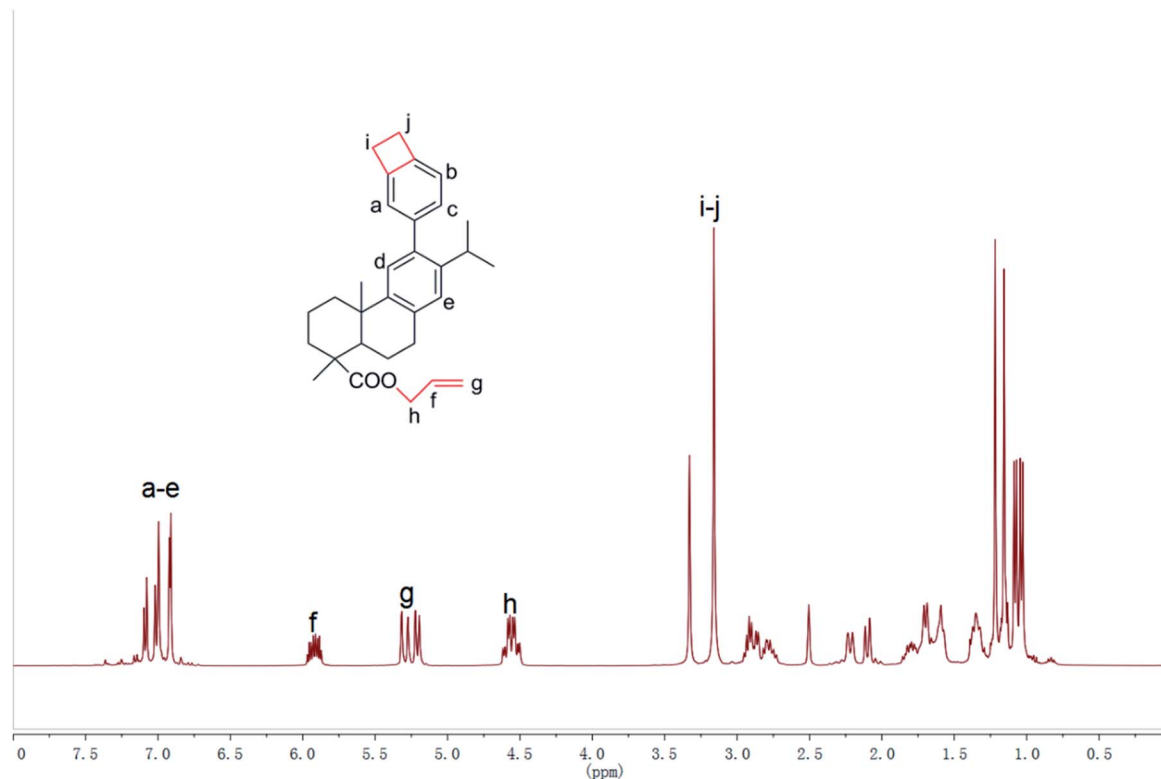
Fig. 1 ^{1}H NMR spectra of the monomer.

exhibiting that the chemical structure of Monomer **3** had been confirmed.

Curing behavior

It is noted that the target monomer can react *via* radical polymerization and ring-opening polymerization, because the monomer contains allyl and benzocyclobutene groups. In order to understand the structural characteristics of Monomer **3**, a DSC trace of monomer with AIBN was carried out, and the results were

shown in Fig. 3. The endothermic peak indicating melting of monomer was observed at 100 °C. In addition, the radical polymerization started at about 103 °C and gave an exothermic peak at the temperature about 123 °C. When the temperature was raised above 200 °C, a broad exotherm was observed, which was attributed to the ring-opening reaction of benzocyclobutene units. The radical polymerization and thermally ring-opening polymerization of Monomer **3** are similar to that of the polymers containing vinyl units and benzocyclobutene groups.[28]
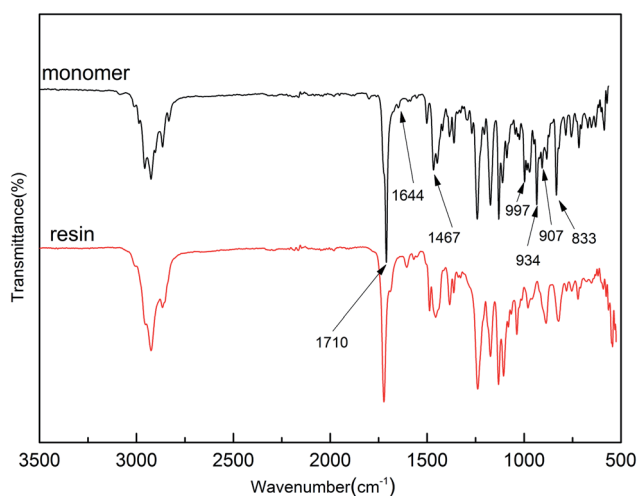

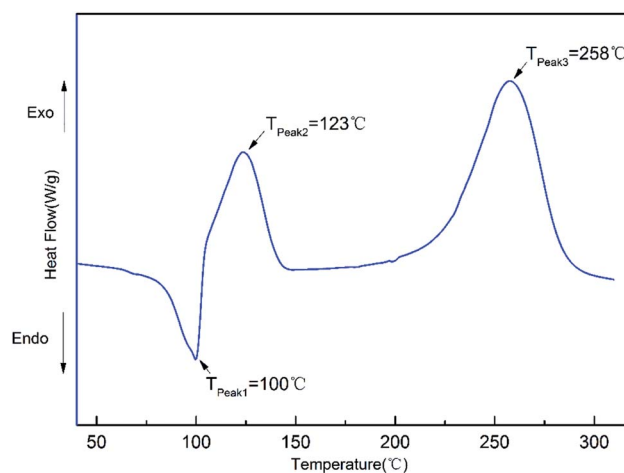Fig. 2 FT-IR spectra of the monomer and resin.

Fig. 3 DSC curve of Monomer **3** at a heating rate of 10 °C min^{-1} in N$_2$.

The polymerization degree of the monomer was also estimated by DSC trace (ESI, Fig. S10†). After the cured resin was maintained at 250 °C for 2 h, the DSC trace indicated that no exothermic peak was observed, suggesting that the polymerization had been completed.

The curing reaction of Monomer **3** was detected by FT-IR spectra. The difference of FT-IR spectra between monomer and cured resin were shown in Fig. 2. In their FT-IR spectra, the characteristic peaks for benzocyclobutene group at 1467, 934, 833 cm^{-1} and the signals for allyl group at 1644, 997, 907 cm^{-1} disappeared after monomer curing. These results suggested that monomer had fully converted to cured resin.

Thermal stability

The thermostability of the cured resin was investigated using thermogravimetric analysis (TGA). The TG and DTG curves for the cured resin are shown in Fig. 4 and 5. The $T_{5\%}$ and $T_{10\%}$ values are chosen as the measure of thermal stability, which represent the temperature at five percent and ten percent mass loss.[21] As shown in Fig. 4, the $T_{5\%}$ and $T_{10\%}$ of the cured resin are 406 °C, 416 °C, respectively. Moreover, the temperature of the highest mass loss occur is 450 °C (Fig. 5). These results indicate that the cured resin has good thermal stability.

Hydrophobic property

Hydrophobic property is an important parameter for the application of high performance material. The hydrophobicity of the cured resin was investigated by the water contact angle test. The water contact angle is measured as 106° (Fig. 6). The result indicates the resin has good hydrophobicity because of the introduction of the hydrogenated phenanthrene ring. As a hydrophobic group, the introduction of the hydrogenated phenanthrene ring can improve the hydrophobicity of polymeric materials.[36,37] The high hydrophobicity is required for the production of devices in the electronics and microelectronics, because it can prevent the moisture adsorption and the deterioration of the dielectric properties effectively.
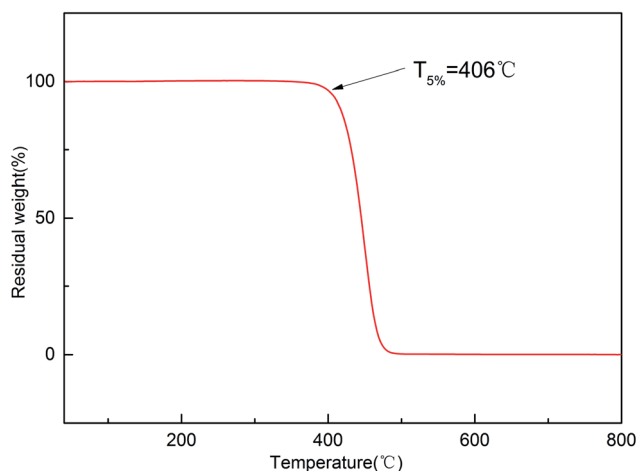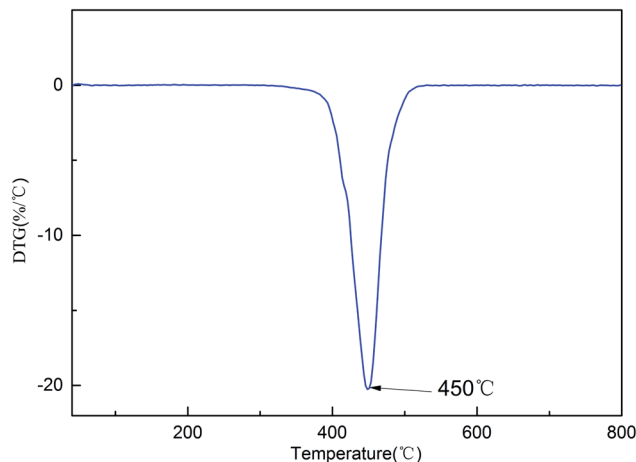

Fig. 5 DTG curve of the cured resin in N$_2$ with a heating rate of 10 °C min^{-1}.

Surface roughness

Some of thermally cross-linked polymers or oligomers showed shrinkage leading to greater surface roughness when they were treated at high temperature, such as epoxy and phenolic resins.[16] However, surface roughness is more crucial for the materials utilized in electronic and microelectronic industry, because low surface roughness implies that the array with high quality can be easily produced on the film surface.[28] In general, the benzocyclobutene-based resin exhibits good surface roughness.[6,19,39] Surface roughness of the polymer castings on a silicon wafer was investigated by atomic force microscopy (AFM). Both planar graph and stereogram are shown in Fig. 7. Measurement results show that the average surface roughness R_a of the cured resin is 0.658 nm in a 5.0 × 5.0 μm^2 area. The good surface roughness indicates that the cured resin is appropriate for application in the electronic and microelectronic fields.[28]

Dielectric properties

The dielectric properties of the cured resin were measured. The results are shown in Fig. 8. As can be seen form Fig. 8, the cured resin shows average dielectric constant (k) of 2.51 and dielectric loss (tan δ) of below 5.0 × 10^{-3} in a range of frequencies varying from 0.1 to 18 MHz at room temperature. These results show

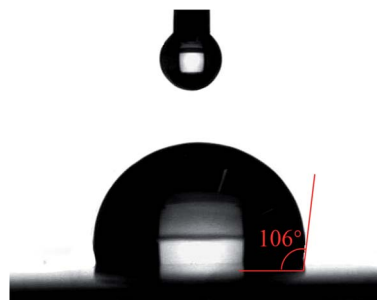**Fig. 4** TG curve of the cured resin in N$_2$ with a heating rate of 10 °C min^{-1}.

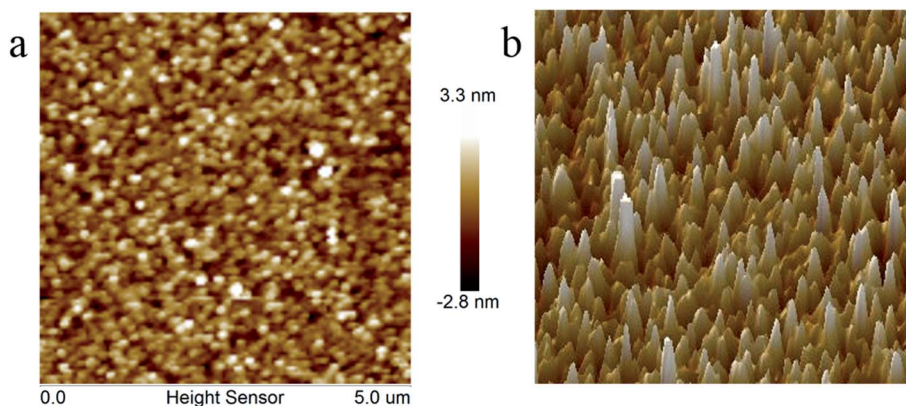**Fig. 6** Contact angle of water on the cured resin.

Fig. 7   AFM images of the cured resin film: (a) planar graph and (b) stereogram.

that the cured resin has excellent dielectric properties. It is noted that the k value of the cured resin is better than the commercially available organic low-k materials, such as poly-imides (3.1–3.4),[40,41] SILK resins (2.65)[42] and polycyanate esters (2.61–3.12).[43]

The reason why the cured resin shows good dielectric properties can be explained by the Debye equation, as shown in eqn (1):[44]

$$\frac{k-1}{k+2} = \frac{4\pi}{3} N \left(\alpha_e + \alpha_d + \frac{u}{3k_b T} \right) \tag{1}$$

where k is dielectric constant, N is the number density of dipoles, α_e is the electric polarization, α_d is the distortion polarization, μ is the orientation polarization related to the dipole moment, k_b is the Boltzmann constant, and T is the temperature. For the cured resin, the bulky hydrogenated phenanthrene ring structure moieties prevented molecular stacking to increase the free volume of the polymer, thus diminishing N. Moreover, the structure is low polar, resulting in the reduction of α_e. Usually, the anisotropy is tiny as to amorphous structure of polymers, as a result, the corresponding μ are small.[44] X-ray diffraction (XRD) patterns (Fig. 9) indicate that the cured resin is essentially amorphous and molecular

stacking is prevented. Thus, the reduction of the three factors (N, α_e and μ) causes the low dielectric constants of the polymer. Moreover, the XRD peak $(2\theta) = 15.5°$ corresponds to the d value of 0.571 nm for the cured resin. The large d spacing indicates the large free volume, endowing the polymer with low k value.[21,44]

Nanoindentation analysis

Nanoindentation was used to examine the mechanical properties of the cured resin by analyzing Young's modulus and hardness.[45] Young's modulus, the most important parameters characterizing mechanical rigidity of materials, can be calculated from eqn (2):[45–47]

$$\frac{1}{E_r} = \frac{1-\nu}{E} + \frac{1-\nu_i}{E_i} \tag{2}$$

where E_i and ν_i are Young's modulus (1141 GPa) and Poisson's rate (0.07) of a diamond indenter, E_r is the reduced elastic modulus, E and ν are Young's modulus and Poisson's ratio of a sample, respectively, and ν is taken as 0.34 for polymer materials.[39] Sample's hardness (H) can be determined by dividing the peak load (P_{max}) by contact area (A), eqn (3):[45–47]
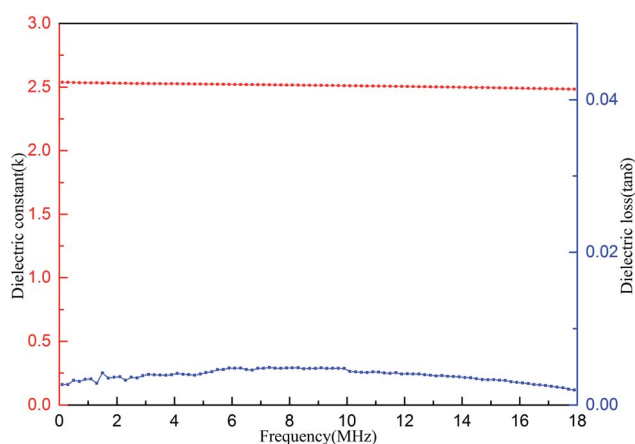

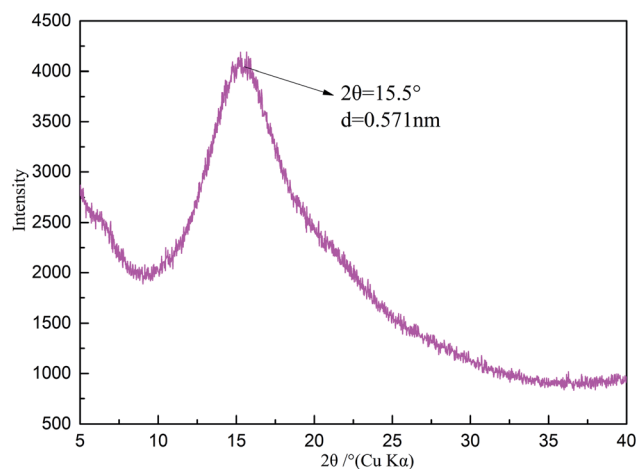Fig. 8   Dielectric constant and dielectric loss of the cured resin.

Fig. 9   X-ray diffraction (XRD) patterns of the cured resin (powder).
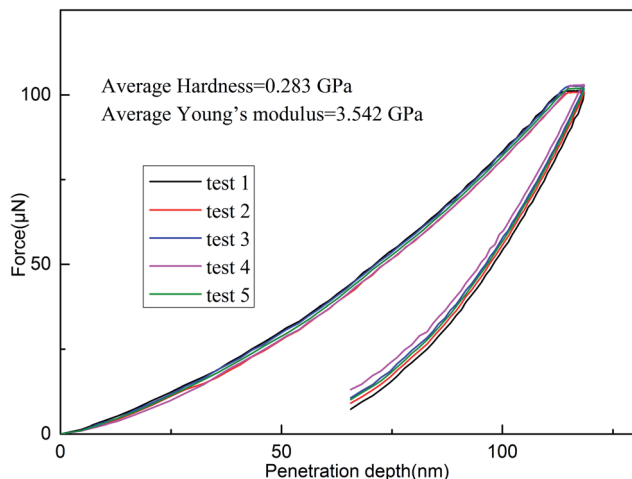
Fig. 10   Results from nanoindentation tests for the cured resin.

$$H = \frac{P_{\max}}{A} \quad (3)$$

As depicted in Fig. 10, the cured resin shows that it has an average hardness of 0.283 GPa and Young's modulus of 3.542 GPa. Those results suggest that the cured resin is satisfactory as the encapsulation resins for integrated circuit dies for application in the microelectronic industry.

Dynamic mechanical properties

The dynamic mechanical properties of the cured resin investigated using Dynamic Mechanical Analysis (DMA). The DMA curves of the cured resin are shown in Fig. 11, the cured resin exhibits high storage modulus with storage modulus at 30 °C of 11.46 GPa. The storage modulus of the resin remains almost unchanged with the increase in temperature in a wide range from 30 to 225 °C. The high storage modulus of the resin is caused by the rigid structural unit of the polymer. Moreover, the glass transition temperature (T_g) of the cured resin is 261 °C, taken as the peak temperature in tan δ curve.
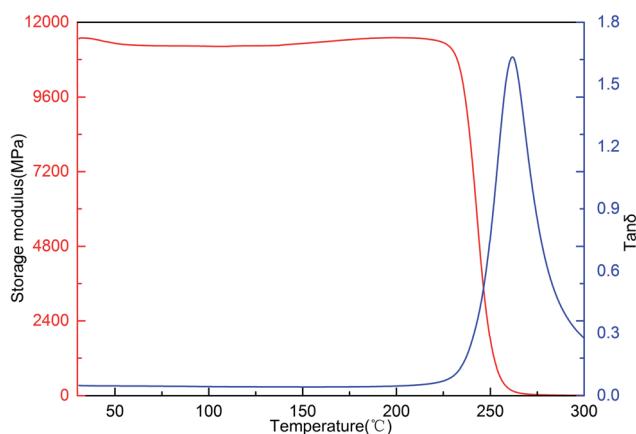

Fig. 11   DMA curves of the cured resin.

Conclusions

In summary, a new thermosetting resin derived from rosin acid has been successfully synthesized. After polymerization at high temperature, the monomer formed an insoluble and infusible polymer. TGA indicated that the polymer had $T_{5\%}$, $T_{10\%}$ of 406 °C and 416 °C, respectively. AFM results indicated that the cured resin had the surface roughness (R_a) of 0.658 nm in a 5.0 × 5.0 μm^2 area, indicating that the polymer film had good surface smoothness and hydrophobicity. Nanoindentation tests and DMA results showed the polymer possessed good mechanical properties, with hardness, Young's modulus and storage modulus of 0.283, 3.54, and 11.46 GPa, respectively. Moreover, the polymer exhibited excellent dielectric properties with average dielectric constant of 2.51 varying from 0.1 to 18 MHz at room temperature. These results indicate that the thermosetting polymer derived from rosin acid is suitable for fields of aerospace, electronics and microelectronics, such as enameled wire varnish, very large scale integrated circuits, fiber reinforced composite materials and interlayer dielectrics in semiconductor packages.

Conflicts of interest

The authors declare no conflict of interest.

Acknowledgements

References

1 J. Tong, S. Diao, K. Jin, C. Yuan, J. Wang, J. Sun and Q. Fang, *Polymer*, 2014, **55**, 3628.
2 Y. Cheng, J. Yang, Y. Jin, D. Deng and F. Xiao, *Macromolecules*, 2012, **45**, 4085.
3 K. Cao, L. Yang, Y. Huang, G. Chang and J. Yang, *Polymer*, 2014, **55**, 5680.
4 L. S. Tan, N. Venkatasubramanian, P. T. Mather, M. D. Houtz and C. L. Benner, *J. Polym. Sci., Part A: Polym. Chem.*, 1998, **36**, 2637.
5 Y. Huang, S. Zhang, H. Hu, X. Wei, H. Yu and J. Yang, *Polym. Adv. Technol.*, 2017, **28**, 1480.
6 C. O. Hayes, P. H. Chen, R. Thedford, C. J. Ellison, G. Dong and C. Willson, *Macromolecules*, 2016, **49**, 3706.
7 Z. J. Wei, Y. W. Xu, L. Zhang and M. M. Luo, *Chin. Chem. Lett.*, 2014, **25**, 1367.
8 A. P. Gies, L. Spencer, N. J. Rau, P. Boopalachandran, M. A. Rickard, K. L. Kearns and N. T. McDougal, *Macromolecules*, 2017, **50**, 2304.
9 J. Yang, S. Liu, F. Zhu, Y. Huang, B. Li and L. Zhang, *J. Polym. Sci., Part A: Polym. Chem.*, 2015, **49**, 381.
10 J. Yang, Y. Cheng and F. Xiao, *Eur. Polym. J.*, 2012, **48**, 751.
11 M. F. Farona, *Prog. Polym. Sci.*, 1996, **21**, 505.

12 Y. Cheng, S. Tian, Y. Shi, W. Chen, Z. Li, T. Zhu and Z. Zhang, *Eur. Polym. J.*, 2017, **95**, 440.

13 Y. Cheng, L. Kong, Z. Ren and T. Qi, *High Perform. Polym.*, 2013, **25**, 980.

14 Y. Huang, S. Zhang, H. Hu, X. Wei, H. Yu and J. Yang, *J. Polym. Sci., Part A: Polym. Chem.*, 2017, **55**, 1920.

15 L. Yang, K. Cao, Y. Huang, G. Chang, F. Zhu and J. Yang, *High Perform. Polym.*, 2014, **26**, 463.

16 S. Tian, J. Sun, K. Jin, J. Wang, F. He, S. Zheng and Q. Fang, *ACS Appl. Mater. Interfaces*, 2014, **6**, 20437.

17 F. He, C. Yuan, K. Li, S. Diao, K. Jin, J. Wang, J. Tong, J. Ma and Q. Fang, *RSC Adv.*, 2013, **3**, 23128.

18 Y. Wang, J. Sun, K. Jin, J. Wang, C. Yuan, J. Tong, S. Diao, F. He and Q. Fang, *RSC Adv.*, 2014, **4**, 39884.

19 Y. Cheng, W. Chen, Z. Li, T. Zhu, Z. Zhang and Y. Jin, *RSC Adv.*, 2017, **7**, 14406.

20 F. He, K. Jin, J. Wang, Y. Luo, J. Sun and Q. Fang, *Macromol. Chem. Phys.*, 2015, **216**, 2302.

21 L. Kong, Y. Cheng, Y. Jin, Z. Ren, Y. Li and F. Xiao, *J. Mater. Chem. C*, 2015, **3**, 3364.

22 X. Zuo, R. Yu, S. Shi, Z. Feng, Z. Li, S. Yang and L. Fan, *J. Polym. Sci., Part A: Polym. Chem.*, 2009, **47**, 6246.

23 J. Wang, C. Lu, Y. Liu, C. Wang and F. Chu, *Ind. Crops Prod.*, 2018, **124**, 244.

24 J. Yu, Y. Liu, X. Liu, C. Wang, J. Wang, F. Chu and C. Tang, *Green Chem.*, 2014, **16**, 1854.

25 X. Yan, Z. Zhai, Z. Song, S. Shang and X. Rao, *Ind. Crops Prod.*, 2017, **108**, 371.

26 C. Lu, J. Yu, C. Wang, J. Wang and F. Chu, *Carbohydr. Polym.*, 2018, **188**, 128.

27 Q. Li, X. Huang, H. Liu, S. Shang, Z. Song and J. Song, *ACS Sustainable Chem. Eng.*, 2017, **5**, 10002.

28 F. He, K. Jin, Y. Wang, J. Wang, J. Zhou, J. Sun and Q. Fang, *ACS Sustainable Chem. Eng.*, 2017, **5**, 2578.

29 V. Singh, S. Joshi and T. Malviya, *Int. J. Biol. Macromol.*, 2018, **112**, 390.

30 P. Carbonell-Blasco, M. M.-M. José and I. Antoniac, *Int. J. Adhes. Adhes.*, 2013, **42**, 11.

31 B. Liu, J. Nie and Y. He, *Int. J. Adhes. Adhes.*, 2016, **66**, 99.

32 R. A. El-Ghazawy, A. M. El-Saeed, H. I. Al-Shafey, A. M. Abdul-Raheim and M. A. El-Sockary, *Eur. Polym. J.*, 2015, **69**, 403.

33 K. Huang, J. Zhang, M. Li, J. Xia and Y. Zhou, *Ind. Crops Prod.*, 2013, **49**, 497.

34 H. Wang, X. Liu, B. Liu, J. Zhang and M. Xian, *Polym. Int.*, 2009, **58**, 1435.

35 H. Wang, H. Wang and G. Zhou, *Polym. Int.*, 2011, **60**, 557.

36 X. Xu, Z. Song, S. Shang, S. Cui and X. Rao, *Polym. Int.*, 2011, **60**, 1521.

37 G. Liu, G. Wu, J. Chen and Z. Kong, *Prog. Org. Coat.*, 2016, **101**, 461.

38 Q. Ma, X. Liu, R. Zhang, J. Zhu and Y. Jiang, *Green Chem.*, 2013, **15**, 1300.

39 K. Ohba, *J. Photopolym. Sci. Technol.*, 2002, **15**, 177–182.

40 G. Maier, *Prog. Polym. Sci.*, 2001, **26**, 3.

41 Y. Watanabe, Y. Shibasaki, S. Ando and M. Ueda, *Polym. J.*, 2006, **38**, 79.

42 S. J. Martin, J. P. Godschalx, M. E. Mills, E. O. S. Ii and P. H. Townsend, *Adv. Mater.*, 2000, **12**, 1769.

43 T. Fang and D. A. Shimp, *Prog. Polym. Sci.*, 1995, **20**, 61.

44 C. Yuan, K. Jin, K. Li, S. Diao, J. Tong and Q. Fang, *Adv. Mater.*, 2013, **25**, 4875.

45 J. Wan, J. Zhao, B. Gan, C. Li, J. Molina-Aldareguia, Y. Zhao, Y. T. Pan and D. Y. Wang, *ACS Sustainable Chem. Eng.*, 2016, **4**, 2869.

46 M. Hardimana, T. J. Vaughanb and C. T. McCarthya, *Compos. Struct.*, 2017, **180**, 782.

47 M. R. Vanlandingham, J. S. Villarrubia, W. F. Guthrie and G. F. Meyers, *Macromol. Symp.*, 2001, **167**, 15.